14th European Conference on Mixing
Warszawa, 10-13 September 2012

PIV STUDY OF MIXING CHARACTERISTICS IN A STIRRED VESSEL WITH A NON-NEWTONIAN FLUID

J.-C. Gabelle[abce], A. Liné[abc], J. Morchain[abc], D. Anne-Archard[d], F. Augier[e]

[a] *Université de Toulouse, INSA; LISBP; 135 Avenue de Rangueil, F-31077 Toulouse, France;*

[b] *INRA UMR792 Ingénierie des Systèmes Biologiques et des Procédés, Toulouse, France ;*

[c] *CNRS, UMR5504, F-31400 Toulouse, France ;*

[d] *IMFT, UMR CNRS/INPT /UPS 5502, Allée du Pr Camille Soula, 31400 Toulouse, France;*

[e] *IFP Energies nouvelles, Rond-point de l'échangeur de Solaize, BP3, 69360 Solaize, France.*

alain.line@insa-toulouse.fr

Abstract. PIV is used to analyze the flow induced by a Rushton turbine in a shear-thinning fluid, at constant input power, constant impeller velocity but different concentrations. The rheology of each shear-thinning fluid is first addressed. The mean velocity fields are compared. POD methodology is applied to estimate coherent structures and turbulence levels. Finally, the heterogeneity of shear rate is estimated and the spatial distribution of dissipation rate of total kinetic energy is addressed.

Keywords: non-Newtonian, POD, mixing, PIV.

1. INTRODUCTION

In the bioprocess industry, stirred tanks are commonly used because they offer high mixing and mass transfer capacities. Depending on the type of micro-organism (e.g. filamentous fungi), fluids of interests usually range from Newtonian to highly viscous non-Newtonian. Because of the scale, bioreactors are performed in turbulent regime or transitional locally. The productivity of this unit operation is often related to the capacity of the reactor to provide good contact area between reactants. Although there have been progress to understand physical mechanisms controlling transport properties, there is still a lack of knowledge that can lead to erroneous design and scale-up.

Much of the most important work on stirred tank hydrodynamics were devoted to the choice of an appropriate stirrer or combination of stirrers to maximise mixing and mass transfer at a global scale [1–4]. Because of the difficulties to study biological media, model fluids are often chosen as they are cheaper and easy to use. A number of articles have been published that investigate in detail the effect of impeller mixing on small scale structures [5–9] but just a few papers concern non-Newtonian fluid [10–12].

The intent of this paper is to identify the flow pattern and characteristic structures in a tank stirred by a Rushton turbine for a non-Newtonian fluid at turbulent and transitional regime (constant power equal to 82 W/m^3, Reynolds numbers equal to 1296, 617 and 303). The experimental work is based on PIV data acquisition of the instantaneous velocity fields. In the impeller steam, the decomposition of flow structures in amplitudes and modes is performed with Proper Orthogonal Decomposition (POD) methodology. This technique

enables to extract mean flow (associated to mode 1) and impeller induced organized structures (associated to modes 2 and 3) from reconstructed velocity fields [13]. The analysis of higher modes is tricky but the statistical analysis of amplitudes of higher modes can point out physical features. Since the fluid is shear-thinning, the heterogeneity of shear rate and local dissipation of kinetic energy are also investigated and compared to volume averaged values.

2. FLOW MEASUREMENTS AND MIXING TANK

2.1 Mixing tank

2D-PIV measurements are performed in a 70 L stirred tank equipped with four equally spaced baffles. A Rushton turbine (D/T = 0.33) is used. The vessel is standard (T=0.45 m), the impeller clearance is C = T/3. More information about the mixing tank dimensions is provided in [7,8,14]. The impeller speed is fixed to 150 rpm.

2.2 PIV system

The PIV system used in this study consisted of a laser and an image acquisition system provided by LaVision (LaVision GmbH, Goettingen, Germany). The system includes a laser Nd-Yag (Quantel, 10 Hz, 200 × 2 mJ), a synchronization system and a Charge-Coupled-Device (CCD) camera (Imager Intense, 12 bits, 1376×1040 pixels^2). Fast Fourier transform (FFT) cross correlation was used to interrogate the two images, which are divided into interrogation area (32×32 or 16×16 pixels^2). For all experiments, 500 to 700 image pairs are recorded and statistical convergence of the velocity is checked. The delay between each frame in an image pair was chosen in relation to the impeller speed and the medium. Four zones in the vessel are investigated: one in the impeller stream, two above and one below. POD is only carried out for the images at the impeller level.

2.3 Working fluid

The shear thinning fluid Zetag7587 (BASF, Ludvigshafen, Germany) is used. It offers good transparency even at high concentration (0.1 to 0.4 %). Rheological measurments were carried out using a Haake Mars III rheometer (ThermoHaake, Germany).

3. RESULTS AND DISCUSSION

3.1 Flow curves

Flow curves of Zetag7587 solutions are presented in Figure 1 for shear rates ranging from 0.001 to 1000 s^{-1}. This three solutions have shear-thining behaviour for the range of shear rates expected in the tank ($\gamma_{MO} = k_s \cdot N = 27.5$ s^{-1}). Rheological data can be fitted to the model of Ostwald de Waele (power law) according to:

$$\mu_a = K \cdot |\dot{\gamma}|^{n-1} \quad (1)$$

with K the fluid consitency factor and n the flow index. The rheological parameters are reporter in Table 1.

Table 1 Rheological parameters fitted to the power law equation.

Fluid	n	K (Pa s^n)	Shear rate range (s^{-1})
Zetag7587 0.1 %	0.422	0.30	1-350
Zetag7587 0.2 %	0.376	0.74	1-600
Zetag7587 0.4 %	0.349	1.65	1-1000

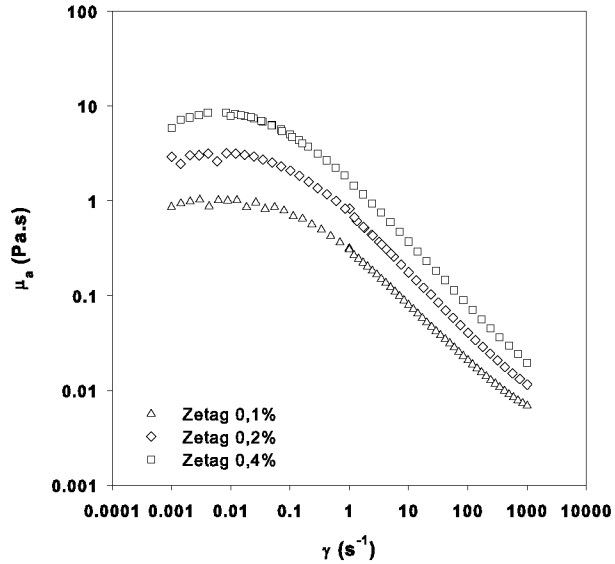

Figure 1 Apparent viscosity of Zetag7587 solutions versus shear rate

3.2 Mean flow

The mean radial and axial velocities normalized with the impeller tip velocity (U_{tip}) are presented in Figure 2 for the fluids tested in this work (at r/R = 1.07).

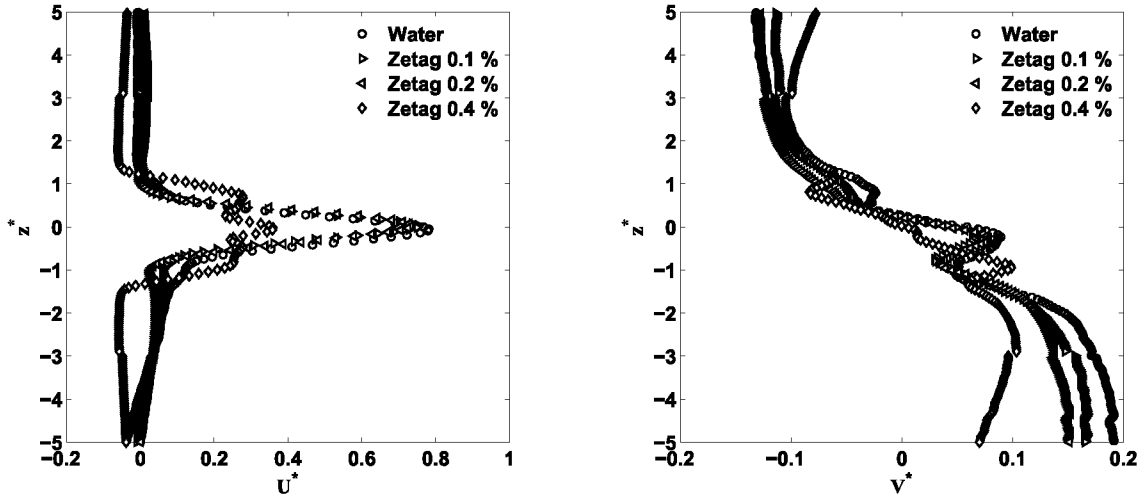

Figure 2 Vertical profiles of normalized mean velocity at r/R = 1.07: (a) radial, (b) axial.

At the higher concentration (0.4%), the vertical profiles of radial and axial velocity differ from the profiles both at lower concentrations and in pure water. This is due to higher viscosity and significantly lower level of turbulence.

3.3 POD

Proper Orthogonal Decomposition (POD) is a linear procedure, which decomposes a set of signals into a modal base [15].We propose in this work to use POD as a complementary analysis tool to identify organized motion in stirred tank [5,6,13,16]. This methodology allows separating the different motions without the necessity to collect angular phased data [13]. POD is carried out using snapshot method with the all set of "non-conditioned" instantaneous velocity fields directly calculated from the measurements. The result is then an orthonormal basis of eigenfunctions and the associated eigenvalues.

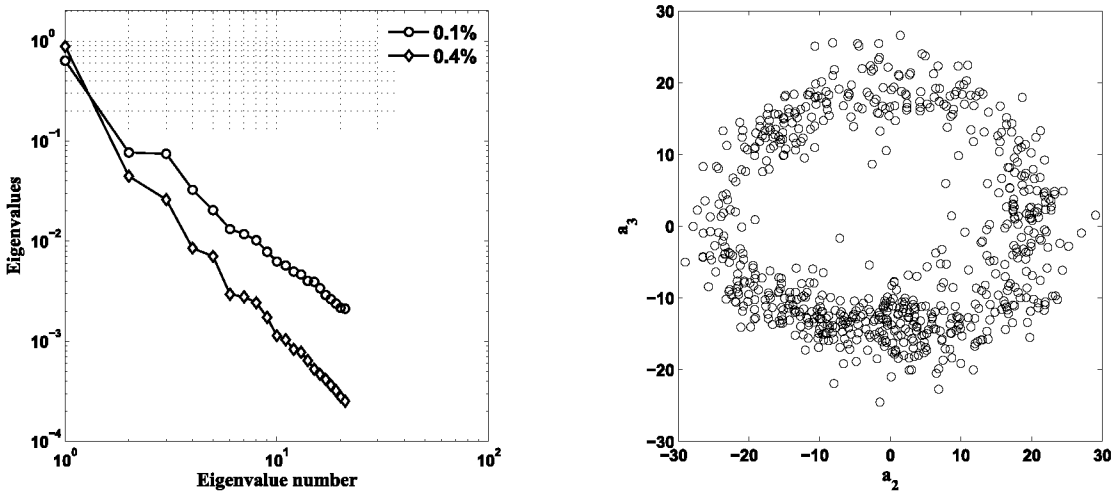

Figure 3 POD characteristics (Zetag): (a) eigenvalues, (b) a_2 and a_3 coefficients

The eigenvalues λ_k are plotted on figure 3.a for two concentrations of Zetag. Clearly, the energy brought by the first mode is a large amount of the total energy (more than 60% and 80 %). Mode 1 is structurally closed to the mean velocity field. The second and third eigenvalues are almost identical involving that the energy brought by these modes is the same. These two modes reveal large scale rotating structures. At the highest Zetag concentration, the turbulence is very weak. The instantaneous velocity field can be projected on each k^{th} POD mode. The value of coefficient a_k deduced from this projection gives a good evaluation of the square root of the energy of the instantaneous flow contained in the corresponding k^{th} mode. The 500 values of the coefficients a_2 and a_3 are plotted on figure 3.b, for the lowest concentration. Clearly, these two modes seem to correspond to a coherent structure ($a_2(\phi)=\sqrt{2\,\lambda_2}\,\sin(\phi)\quad a_3(\phi)=\sqrt{2\,\lambda_3}\,\sin(\phi)\quad with\ \lambda_2 \approx \lambda_3$). From these projections, it is possible to reconstruct the velocity field. In particular, one can reconstruct the mean flow (first mode), the organised motion (second and third modes) and the turbulence (higher modes). The vertical profiles of turbulent, organised and total fluctuating kinetic energy are plotted on figure 4.

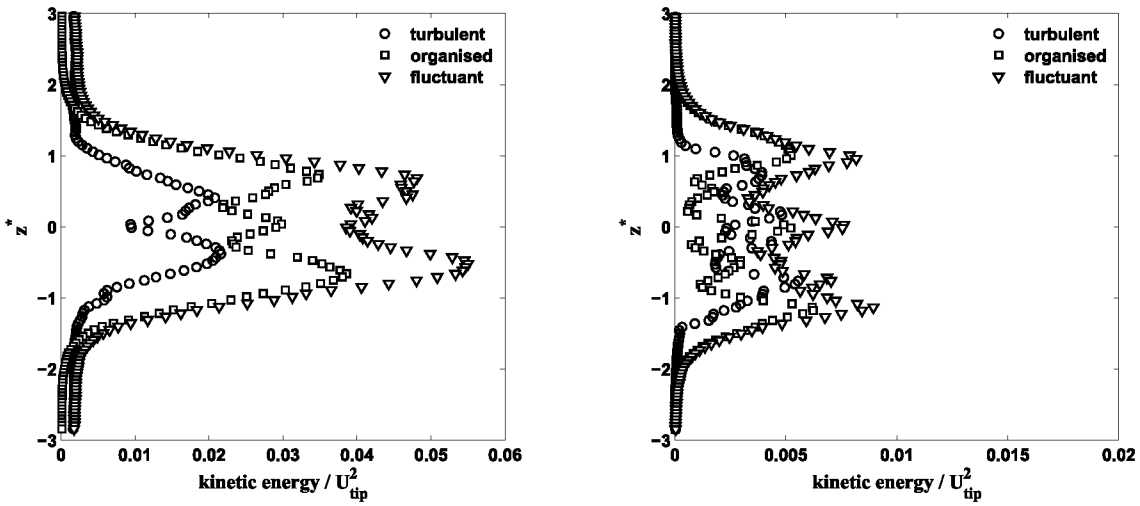

Figure 4 vertical profiles of kinetic energy components at a radial position close to the impeller tip (organized flow, turbulent flow and total fluctuating flow) (Zetag): (a) 0.1%, (b) 0.4%

One can see on figure 4.a, that at the lowest concentration (0.1%), the organised motion contains slightly higher kinetic energy than the turbulence; however, the organised motion is restricted to the impeller zone. At the higher concentration (0.4%), the organised motion associated to modes 3 and 4 is close to the total kinetic energy; in this case, the so-called turbulent kinetic energy may be attributed to additional organised motions corresponding to modes 4 and 5 that are coupled and look very similar in terms of energy (see figure 3.a).

4. CONLUSION AND DISCUSSION

Based on PIV data, the mean flow can be estimated. POD enables to discriminate between coherent organized motion and turbulence. The last issue is to analyze the heterogeneity of shear rate at different Zetag concentrations. The spatial distributions of total shear rates are plotted on figure 5. The maximum values of the shear rate are 500 s^{-1} and 250 s^{-1}, respectively at 0.1% and 0.4%.

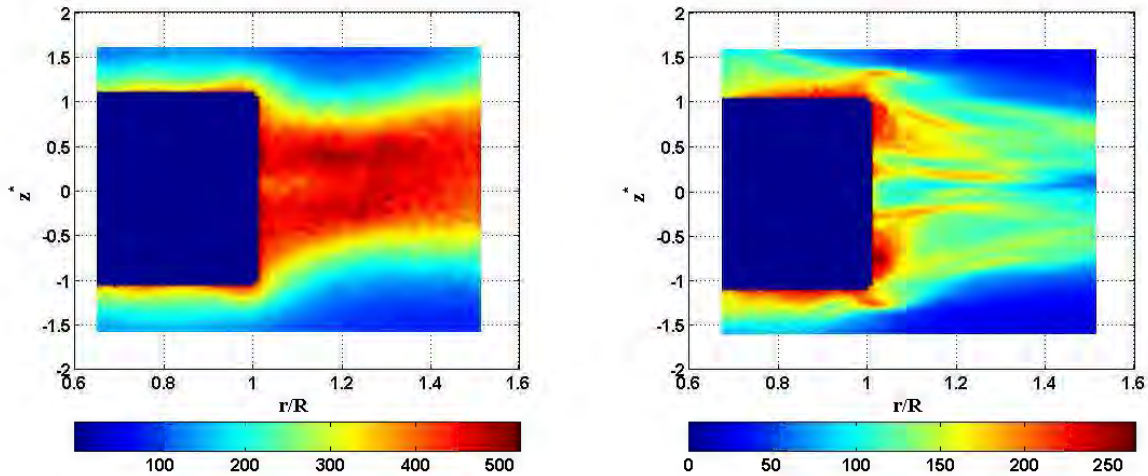

Figure 5 Spatial distributions of total shear rates: (a) 0.1%, (b) 0.4%.

The shear rate heterogeneity will impact the apparent viscosity of the shear-thinning fluid. Figure 1 and Table 1 enable to estimate this viscosity and to deduce the spatial distribution of dissipation rate of kinetic energy (Figure 6). The maximum values of dissipation rate are close to 2.5 W/kg which is large (30 times) compared to their global value close to 0.082 W/kg.

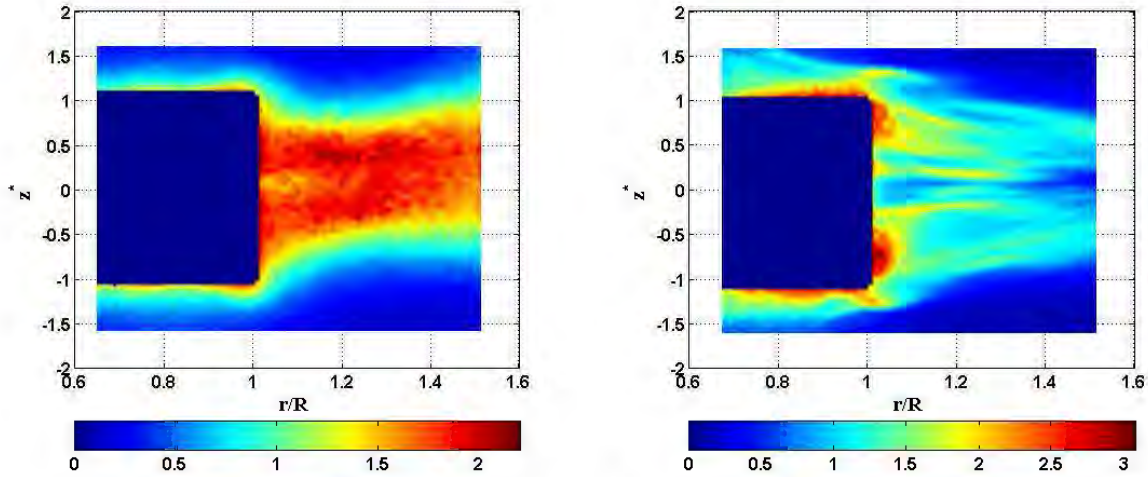

Figure 6 Spatial distributions of dissipation rate of kinetic energy in W/kg (a) 0.1%, (b) 0.4%.

ACKNOWLEDGMENT

This work was supported by the French Environment and Energy Management Agency (ADEME) and IFP Energies Nouvelles.

REFERENCES

[1] Albaek M. O., Gernaey K. V., and Stocks S. M., 2008, "Gassed and ungassed power draw in a pilot scale 550 litre fermentor retrofitted with up-pumping hydrofoil B2 impellers in media of different viscosity and with very high power draw," Chemical Engineering Science, **63**(24), pp. 5813–5820.

[2] Nienow A. W., 1990, "Gas dispersion performance in fermenter operation," Chemical Engineering Progress, **86**(2), pp. 61–71.

[3] Gabelle J. - C., Augier F., Carvalho A., Rousset R., and Morchain J., 2011, "Effect of tank size on kLa and mixing time in aerated stirred reactors with non - newtonian fluids," The Canadian Journal of Chemical Engineering, **89**(5), pp. 1139–1153.

[4] Pedersen A. G., Bundgaardnielsen M., Nielsen J., and Villadsen J., 1994, "Characterization of mixing in stirred tank bioreactors equipped with rushton turbines," Biotechnology and Bioengineering, **44**(8), pp. 1013–1017.

[5] Ducci A., Doulgerakis Z., and Yianneskis M., 2007, "Decomposition of Flow Structures in Stirred Reactors and Implications for Mixing Enhancement," Ind. Eng. Chem. Res., **47**(10), pp. 3664–3676.

[6] Doulgerakis Z., Yianneskis M., and Ducci A., 2011, "On the Manifestation and nature of macroinstabilities in stirred vessels," AIChE Journal, **57**(11), pp. 2941–2954.

[7] Escudié R., and Liné A., 2003, "Experimental analysis of hydrodynamics in a radially agitated tank," AIChE Journal, **49**(3), pp. 585–603.

[8] Escudié R., and Liné A., 2006, "Analysis of turbulence anisotropy in a mixing tank," Chemical Engineering Science, **61**(9), pp. 2771–2779.

[9] Gabriele A., Nienow A. W., and Simmons M. J. H., 2009, "Use of angle resolved PIV to estimate local specific energy dissipation rates for up- and down-pumping pitched blade agitators in a stirred tank," Chemical Engineering Science, **64**(1), pp. 126–143.

[10] Arratia P. E., Kukura J., Lacombe J., and Muzzio F. J., 2006, "Mixing of shear - thinning fluids with yield stress in stirred tanks," AIChE Journal, **52**(7), pp. 2310–2322.

[11] Venneker B. C. H., Derksen J. J., and Van den Akker H. E. A., 2010, "Turbulent flow of shear-thinning liquids in stirred tanks—The effects of Reynolds number and flow index," Chemical Engineering Research and Design, **88**(7), pp. 827–843.

[12] Koutsakos E., and Nienow A. W., "Effects of rheological properties of simulated fermentation broths on flows in stirred bioreactors: a Laser Anemometry study," Rheology of food, pharmaceutical and biological materials with general rheology, Carter, R. E., pp. 284–302.

[13] Moreau J., and Liné A., 2006, "Proper orthogonal decomposition for the study of hydrodynamics in a mixing tank," AIChE Journal, **52**(7), pp. 2651–2655.

[14] Escudié R., Bouyer D., and Liné A., 2004, "Characterization of trailing vortices generated by a Rushton turbine," AIChE Journal, **50**(1), pp. 75–86.

[15] Lumley J. L., 1967, "The structure of inhomogeneous turbulence," Atmospheric Turbulence and Wave Propagation, A. M. Iaglom and V.I. Tatarski, pp. 166–178.

[16] Tabib M. V., and Joshi J. B., 2008, "Analysis of dominant flow structures and their flow dynamics in chemical process equipment using snapshot proper orthogonal decomposition technique," Chemical Engineering Science, **63**(14), pp. 3695–3715.